**ADVANCED
MATERIALS
INTERFACES**

Supporting Information

Mg Deficiency in Grain Boundaries of n-Type Mg_3Sb_2 Identified by Atom Probe Tomography

Jimmy Jiahong Kuo, Yuan Yu, Stephen Dongmin Kang, Oana Cojocaru-Mirédin, Matthias Wuttig, and G. Jeffrey Snyder*

Supporting Information: Mg deficiency in grain boundaries of n-type Mg_3Sb_2 identified by atom probe tomography

Jimmy Jiahong Kuo,[†] Yuan Yu,[‡] Stephen Dongmin Kang,[†,¶] Oana Cojocaru-Mirédin,[‡] Matthias Wuttig,[‡] and G. Jeffrey Snyder[*,†]

[†]*Northwestern University, Evanston, IL 60208, USA*

[‡]*I. Physikalisches Institut (IA), RWTH Aachen, 52074, Aachen, Germany*

[¶]*California Institute of Technology, Pasadena, CA 91125, USA*

E-mail: jeff.snyder@northwestern.edu

Sb deficiency in the bulk

In the bulk region, the detected concentration of Sb is slightly lower than the nominal one (*i.e.,* 40%) can be due to two reasons. (a) Sb show very high probability of multiple events. Some fragments might be lost due to the 'dead time' and 'dead zone' effect of the detector;[1] (b) Large Sb clusters also show molecular dissociation, which causes composition deviations. As these factors also affect the boundary region, we focus on the concentration difference rather than its absolute value.
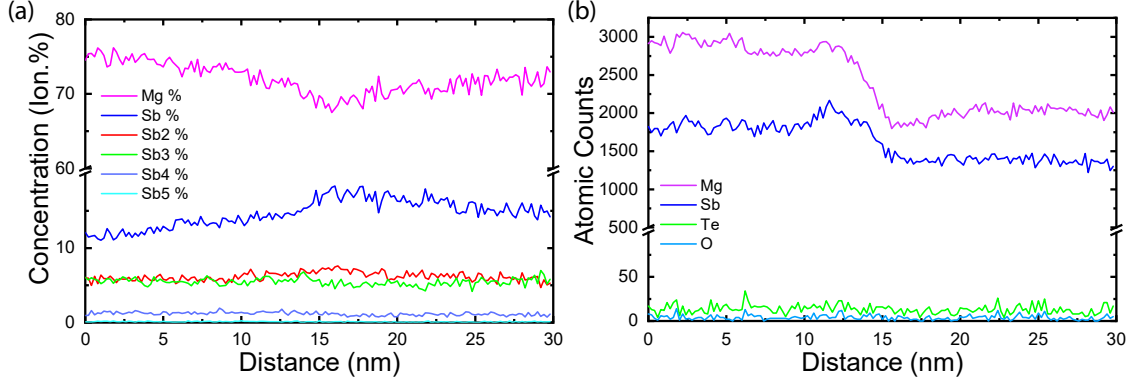
Figure S1: (a) Atomic concentrations analysis of Sb clusters across the 2D defect. Peaks of concentration from single Sb ions and Sb_2 clusters can be identified near the 2D defect, while larger clusters shows negligible variation of concentration. (b) Atom counts for each element. The different counts across the defect can be resulted from different evaporation rates due to their crystal orientation.

Sb clusters

Another compound-specific factor, formation of Sb clusters, doesn't affect our observation as well. In the literature, group V elements have been observed to evaporate as clusters due to their higher evaporation field.[2,3] Migration of clusters on the surface of tip as well as undetected clusters (*e.g.*, Sb_6 and so on) with large mass-to-change ratios can result in an inaccurate atomic concentrations. In contrast to this concern, Fig. S1 (a) shows that the spacial variation of Sb concentration is mainly contributed from single Sb ions and Sb_2 clusters. Any undetected or migrating large Sb clusters therefore most likely contribute uniformly to the concentration profile.

Zone line

The zone line[4] is a 2D low-density region formed due to trajectory aberration of different crystallographic orientations. In Fig.S1 (b), a change of atom count across the 2D defect can be observed due to different evaporation rates associated with their crystal orientations. Within the defect region, the atom count showing a relatively smooth transition suggests that the feature is not a zone line. Furthermore, the constant atom counts within each grain

further confirms the existence of a 2D defect. Similar Mg deficiency observed from another tip (see SI) also clarifies the concern of zone line, as its formation is sensitive to crystal orientations with respect to the tip. Note that the measurement was done by a different instrument and was able to include larger Sb clusters (*e.g.*, Sb_6 and Sb_7). Based on these augment, we verify the validity of the observation of 2D defects with Mg deficiency in n-type Mg_3Sb_2 compounds.
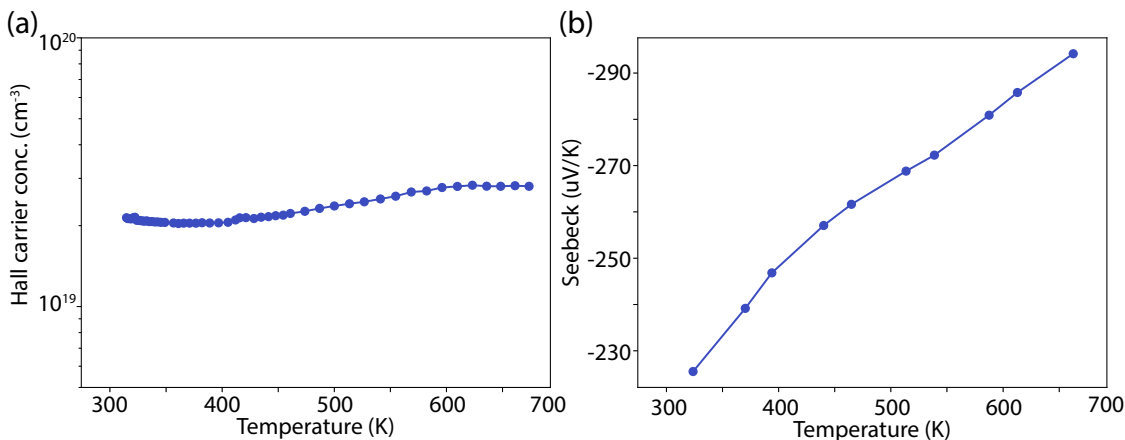

Figure S2: Measurement of (a) Hall carrier concentration and (b) Seebeck coefficient. The results show that the sample is a degenerate n-type Mg_3Sb_2.

Measurement of electrical n-type properties

Fig. S2 shows the n-type properties of the sample. The Hall coefficient measurements were determined using the 4-point probe Van der Pauw technique with a 0.8 T magnetic field under high vacuum.[5] The Seebeck coefficients of the samples were obtained using chromel-Nb thermocouples by applying a temperature gradient across the sample to oscillate between ± 5 K.[6]
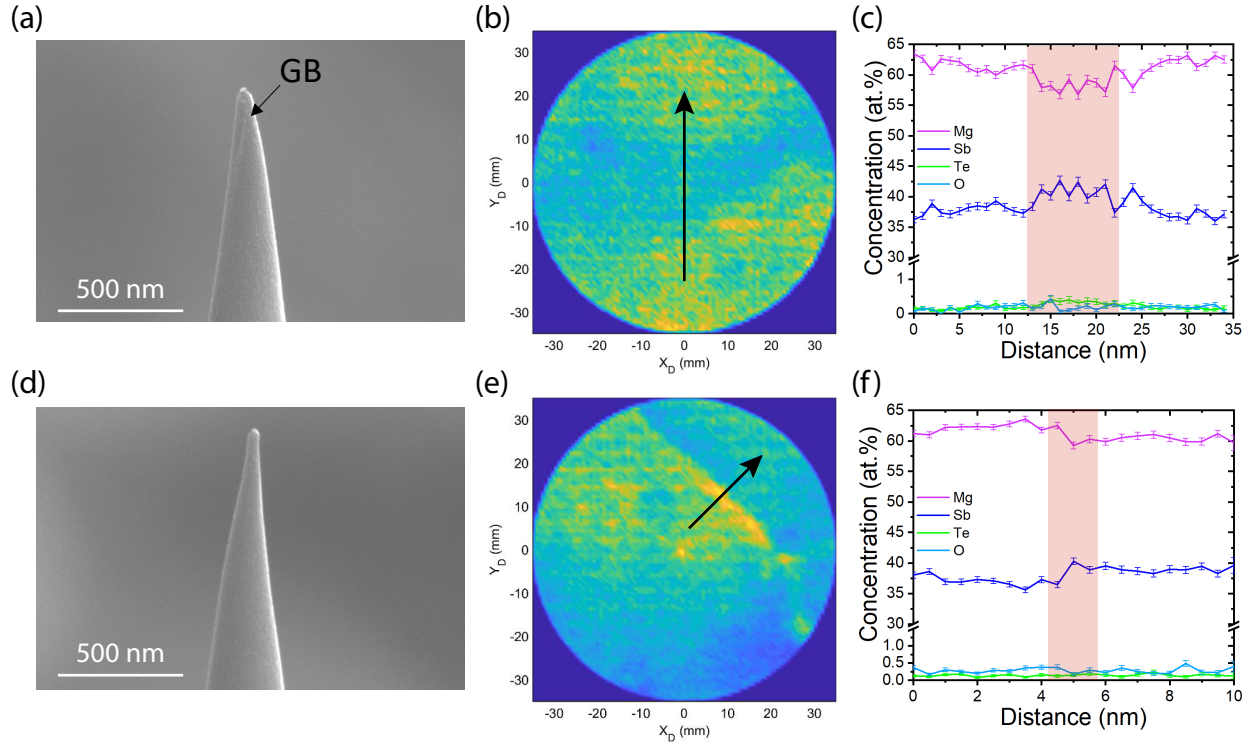
Figure S3: (a)SEM image of the APT specimen. Radius of the tip is estimated to be smaller than 50 nm. A grain-boundary-like structure is visible in the image. (b) Atomic density maps near the bottom of the tip. A low-density 2D defect can be observed. (c) Atomic concentrations analysis along the arrow direction in (b).The profile is constructed from a cylinder region-of-interest (diameter: 20 nm, length: 35 nm, and bin size: 1 nm).The red area corresponds to the grain-boundary region. The defect shows a Mg deficient profile across the 2D defect, while impurities (*e.g.,* O and Te) show little variation across the defect. (e)-(f) corresponds to data from another APT specimen which does not show a clear Mg deficient profile across the grain boundary as the other two APT specimens. This can be due to structural details (*e.g.,* mis-orientation angle) of the defect affect the degree of stoichiometric deviation.

Additional data

Fig. S3(a)-(c) shows another APT specimen with a 2D defect that shows a Mg-deficient concentration profile across the defect. On the other hand, Fig. S3(d)-(f) corresponds to another specimen which doesn't show a clear Mg-deficient profile. We suspect that the structural details (*e.g.,* mis-orientation angle) of the defect affect the degree of stoichiometric deviation. These measurements were performed using a different instrument and setup: LEAP 4000X Si, 355 nm, 50 K, 10 pJ, 200 kHz, detection rate of 5 ions per 1000 pulses and

detector efficiency of 50%.

References

(1) Peng, Z.; Vurpillot, F.; Choi, P.-P.; Li, Y.; Raabe, D.; Gault, B. On the detection of multiple events in atom probe tomography. *Ultramicroscopy* **2018**, *189*, 54–60.

(2) Liddle, J.; Norman, A.; Cerezo, A.; Grovenor, C. Pulsed laser atom probe analysis of ternary and quaternary III-V epitaxial layers. *Le Journal de Physique Colloques* **1988**, *49*, C6–509.

(3) Gorman, B. P.; Norman, A. G.; Yan, Y. Atom probe analysis of III–V and Si-based semiconductor photovoltaic structures. *Microscopy and Microanalysis* **2007**, *13*, 493–502.

(4) Riley, J. R.; Bernal, R. A.; Li, Q.; Espinosa, H. D.; Wang, G. T.; Lauhon, L. J. Atom probe tomography of a-axis GaN nanowires: analysis of nonstoichiometric evaporation behavior. *ACS nano* **2012**, *6*, 3898–3906.

(5) Borup, K. A.; De Boor, J.; Wang, H.; Drymiotis, F.; Gascoin, F.; Shi, X.; Chen, L.; Fedorov, M. I.; Müller, E.; Iversen, B. B.; Snyder, G. J. Measuring thermoelectric transport properties of materials. *Energy & Environmental Science* **2015**, *8*, 423–435.

(6) Iwanaga, S.; Toberer, E. S.; LaLonde, A.; Snyder, G. J. A high temperature apparatus for measurement of the Seebeck coefficient. *Review of Scientific Instruments* **2011**, *82*, 063905.